X-ray $K\alpha$ satellites of copper

Nissan Maskil and Moshe Deutsch
Physics Department, Bar-Ilan University, Ramat-Gan, Israel
(Received 20 April 1988)

The supra-$K\alpha_1$ satellite spectrum of Cu was measured using a high-resolution monolithic-double-crystal spectrometer. Its total intensity relative to that of the $K\alpha_1$ line was found to be 6×10^{-3}, in good agreement with the only published measurement and the theoretical predictions. The spectrum includes fine structure. Relativistic Dirac-Fock (RDF) and nonrelativistic Hartree-Fock calculations were carried out and compared with the measured data in detail. The RDF calculations allow assignment of all seven structural features detected in the measured spectrum to $2p$-spectator-hole transitions, with a possible small contribution from $2s$-spectator-hole transitions. The new line assignments are discussed and compared to earlier work. Similar measurements were also done in the energy range between the $K\alpha_1$ and $K\alpha_2$ lines. Only one possible feature, on the limit of statistical significance, was found close to the energy predicted for a radiative Auger transition involving a $3d$ electron. Its relative intensity, 5×10^{-4}, is much lower than predicted theoretically but within a factor of 2 from recent measurements of equivalent electron-capture-excited transitions.

I. INTRODUCTION

X-ray satellite lines were recognized[1] as early as 1921 to originate from single electronic transitions, $1s^{-1}\rightarrow 2p^{-1}$, in the presence of a $2p^{-1}$ or $2s^{-1}$ spectator hole. Such transitions, which involve more than one electron of the same atom, are able, in principle, to yield information on electron-electron correlations and excitation dynamics in atoms.[2,3] Thus, they provide the basis for a first step beyond the conventional single-electron fixed-potential models of atomic excitations. The experimental accessibility of such processes is, however, severely restricted by the very low cross sections, which, for two-electron processes in medium-z atoms are of order 10^{-3} of that of single-electron ones. High-resolution measurements of these processes by x-ray absorption spectroscopy were made possible only recently[3] by using the high x-ray fluxes provided by synchrotron sources. Although emission spectroscopy fared somewhat better, for the iron-group transition metals, a testing ground of choice for atomic-structure theories, the only systematic study available of the $K\alpha$ satellite spectrum is the pioneering work of Parratt[4] published more than 50 years ago and restricted to energies above the $K\alpha_1$ line. It should be noted that the hypersatellite and correlated hypersatellite spectra of several iron-group elements were recently studied by Salem and co-workers,[5] and large deviations from theoretically predicted cross sections were found. For Cu, the subject of this study, only two other partial studies of the satellite spectrum are available. Edamoto's[6] measurements are restricted to wavelengths only and, due to the film technique used, beset by serious limitations as discussed by Parratt.[4] Edwards and Langford[7] used the measured spectrum for assessing spectrometer resolution effects, but otherwise no analysis, such as resolution into separate lines or transition assignments, is provided.

We have therefore undertaken to measure the $K\alpha$ satellite spectrum of Cu at energies both above and below the $K\alpha_1$ line using a stable, high-resolution monolithic-double-crystal spectrometer (MDCS), described in Sec. II. In Sec. III the data obtained for each energy range are discussed separately. For the high-energy region a good agreement is found for the total width and relative cross section of the satellite spectrum with Parratt's measurements and theoretical predictions.[8,9] A phenomenological resolution of the spectrum into individual lines, as suggested by Parratt, is presented as well as a comparison with published theoretical studies[10,11] and our detailed relativistic Dirac-Fock and nonrelativistic Hartree-Fock calculations. Based on these comparisons, new line assignments are suggested for several features resolved here for the first time. In the low-energy region only a single line is found, assignable to a radiative Auger transition predicted to lie in this region. In Sec. IV suggestions for further work are presented.

II. EXPERIMENTAL

As the MDCS has been fully discussed elsewhere[12,13] we will give here only a brief description. This device is cut entirely from a single block of dislocation-free, perfect silicon crystal. The roles of the two separate crystals of a conventional spectrometer are played here by two different sets of Bragg planes of the same crystal. Energy tuning is done by rotating the device by some angle α about an axis perpendicular to the first set of planes. This changes the effective angle of incidence of the beam emerging from the first set of planes onto the second one. The monolithic structure of the MDCS ensures perfect relative alignment of the two "crystals" and eliminates almost all the delicate alignment arrangements and procedures required in a conventional high-resolution spec-

trometer. It also greatly enhances stability and provides high immunity to vibrations, temperature variations, etc. This is crucial for the long data collection runs dictated by the low intensity of the satellite lines. Furthermore, as the energy transmission function of the MDCS is an even function of the angle of rotation α, a single emission line will produce two peaks in the spectrum: one for, say, $+\alpha_p$ and one for $-\alpha_p$. This allows $\alpha=0$, and hence the absolute energy, to be determined accurately and also immediately identifies as spurious spectral features not appearing in both peaks. This property is of great importance when trying to identify weak satellite lines on the flanks of intense diagram ones.

The actual MDCS used, employs the (135) and ($\bar{1}\bar{3}5$) planes. In the energy range of interest here its angular dispersion for α rotations is ~ 1 eV/deg. While the intrinsic energy resolution of the MDCS is determined by the width of the reflection curves of the Bragg planes used and is of order 10^{-2} eV, the restrictions on incident beam divergence were relaxed to give an overall energy resolution of 0.5 eV for the sake of increasing the count rate. This resolution is still negligibly small compared with the ~ 13 eV width of the satellite complex. The inherent absolute energy accuracy of the MDCS is of order 1 ppm. The radiation source was a sealed Cu x-ray tube run off a stabilized constant potential Picker x-ray generator, operating at 30 kV and 16 mA. Temperature variations during measurement were less than $\pm 0.5\,^{\circ}$C. For further details see Ref. 13.

III. RESULTS AND DISCUSSION

Measurements were carried out at energies both above and below the $K\alpha_1$ line. The results obtained for each region will now be discussed separately.

A. High-energy region

The supra-$K\alpha_1$ satellite spectrum was measured over the range 8048–8096 eV. The contribution from the flanks of the $K\alpha_1$ line was subtracted using a two-Lorentzian representation the widths, positions and relative intensities of which were obtained from the high-resolution study of the diagram lines in Ref. 13. Their absolute intensity was adjusted by least-squares fitting to the present data at energies above and below the satellite complex. A constant background was also included in the fit and subtracted along with the two Lorentzians. The spectrum so obtained was used in the subsequent data analyses and is shown in Fig. 1.

The shape of the spectrum indicated four underlying lines: two at the center and one to each side of it. Thus, following Parratt,[4] the spectrum was phenomenologically resolved into four lines denoted by α', α_3, α_4, and α_3', using nonlinear least-squares computer fits. As the lines are highly overlapping no clear clues as to their shape are provided by the spectrum itself. While the fast decrease in intensity at the edges favors Gaussian line shapes, only a slight change ($\leq \frac{1}{2}\sigma$, where σ is the standard deviation of the raw data) in the fitted background was required to obtain an almost equally good fit for Lorentzian line shapes. Thus, both line shapes were examined allowing, in each fit, a variation of height, position, and width of each line. The results are summarized in Table I along with earlier measurements and theoretical predictions. The assignments in the table of our theoretical transitions to the resolved lines are discussed below. The resolved spectrum is shown in Fig. 1.

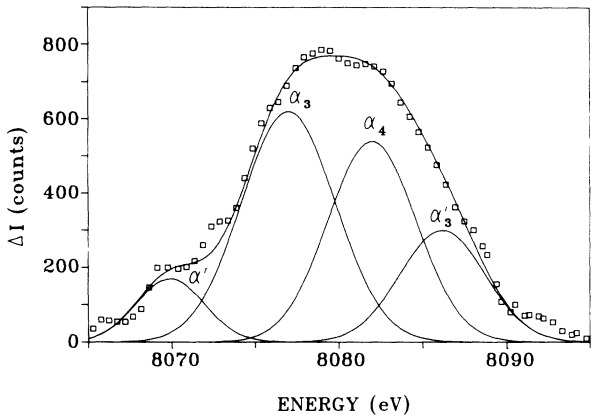

FIG. 1. $K\alpha$ satellite spectrum of copper. The contributions from the flanks of the $K\alpha_1$ line are subtracted as discussed in the text. Following Parratt (Ref. 4), the measured spectrum (□) is resolved into four individual Gaussians (——), the sum of which closely fits the data. For positions, widths, and intensities see Table I.

As pointed out by Parratt, the resolution of the satellite spectrum into individual lines is prone to large uncertainties in the parameters extracted, due to the large widths and degree of overlap of the individual lines. The uncertainty in the positions and width of the resolved lines is estimated to be ~ 1 eV and in the relative intensities 20%. Within these limits there is an overall agreement among all measured data sets, although some differences in details do occur. Cauchois' wavelengths[14] agree best with ours, while those of Parratt seem to be consistently higher than ours by ~ 1 eV. This may result from an inaccurate calibration of his absolute energy scale, whereas ours is directly related to the silicon lattice constant and is accurate to 1 ppm.[12,13] As Edamoto's absolute wavelength calibration results on Parratt's values, his results are also shifted correspondingly. In addition, his data seems to deviate increasingly with energy from the other sets. This may result from an aberration in his photographically recorded data or in the densitometer used for its digitization.

The linewidths of our Gaussian model are in excellent agreement with the only other available data, Parratt's. The Lorentzian widths agree somewhat less but still within the combined error. The same holds for the relative intensities with the exception of the α' line which in our data is much stronger than is Parratt's. As this is the weakest and narrowest line of the spectrum, it is doubtful that this difference has any significance. There is also a reversal in the relative intensities of the α_3 and α_4 lines between Parratt's measurements and ours. In the former

TABLE I. The resolved satellite lines. E, energies in eV; RI, intensities relative to that of the $K\alpha_1$ line, in units of 10^{-3}; W, full width at half maximum in eV. Note the good agreement between present Gaussian data and Parratt's measurements. For a discussion of line assignments for the various theoretical calculations see text and Table III.

Source	Total complex RI	Total complex W	α' E	α' RI	α' W	α_3 E	α_3 RI	α_3 W	α_4 E	α_4 RI	α_4 W	α_3' E	α_3' RI	α_3' W
						Experimental								
Present work														
Lorentzian	8.9	13.3	8069.7	0.46	4.2	8077.5	4.2	7.6	8082.4	3.5	7.3	8086.6	0.75	4.8
Gaussian	6.0	12.6	8069.9	0.49	4.8	8077.0	2.4	6.6	8082.0	2.0	6.2	8086.2	1.1	6.0
Ref. 4	6.0	12.2	8070.9	0.08	4.0	8078.5	2.2	5.7	8083.1	2.7	6.4	8087.5	1.0	6.6
Ref. 6			8070.4			8079.2			8084.0			8080.3		
Ref. 7	8.6	13.5												
Ref. 14			8070.75			8078.2			8082.4			8087.2		
						Theoretical								
Present work														
RDF			8069.7			8081.1			8083.0			8085.6		
			8067.7			8080.7								
HF			8070.0			8081.5			8084.2			8087.6		
			8070.3			8084.7								
Ref. 10			8070.6			8079.2			8082.1			8087.6		
						8079.6			8082.4					
Ref. 8	6.2													
Ref. 9	5.8													

the α_4 line is more intense by 18% than the α_3, while in the later α_3 is more intense than α_4 by 20%, for both Lorentzian and Gaussian line shapes. It is difficult to assess whether this difference is an artifact due to the different resolution procedures employed or a real effect. However, our relativistic calculations discussed below yield a similar 25% intensity excess for the α_3 line, over that of α_4. The reversed α_3/α_4 intensity ratio which seems to be given by the Hartree-Fock (HF) calculation holds only in the LS coupling scheme. As calculated relative intensities depend very strongly on the coupling scheme[11] and as the appropriate one for Cu is intermediate, not LS coupling, no real contradiction exists.

The intensity of the complete satellite spectrum relative to that of the $K\alpha_1$ line calculated using the Gaussian line shapes is in excellent agreement with Parratt's measurements. It also agrees well with Richtmyer's[8] hydrogenic wavefunction, single screening constant calculations, and Aberg's[9] shake-up predictions. The slower decreasing Lorentzian lineshapes yield a higher relative intensity, close to that of Edwards and Langford.[7] While on grounds of a somewhat better fit of the spectrum by Gaussian lineshapes we feel that the Lorentzian-derived total intensity overestimates the actual cross section, no clear-cut conclusion to this effect emerges from the analysis. A relative intensity of $(7.4\pm1.5)\times10^{-3}$ is suggested, therefore, for the total satellite complex.

The measurements were supplemented by intermediate-coupling HF (energies only) and relativistic Dirac-Fock (RDF) (both energies and intensities) calculations for the $1s^{-1}2s^{-1}\rightarrow 2s^{-1}2p^{-1}$ and $1s^{-1}2p^{-1}\rightarrow 2p^{-2}$ transitions. A ground state with a missing $4s$ electron was assumed for the metal-bound Cu atom[12] and the well-known deviation of the calculated K-level energy from the experimental one was corrected for by using the difference between the measured $K\alpha_1$ energy and each of the calculated ones.[11] The HF calculations were done using single-configuration HF energies and Slater integrals obtained from the MCHF code of Froese Fischer[15] and the calculated two-electron spin-orbit parameters ζ were scaled[11] by the ratio of the measured to calculated one $(2p^{-1})$ electron ζ. The RDF calculations employed the MCDF code of Grant *et al.*[16] in the extended average-level optimization scheme, and included first-order Breit, self-energy, and a second-order vacuum-polarization contributions to the energy levels. The results obtained for the various transitions are given in Table II, along with the semiempirical nonrelativistic calculated energies of Nigam and Soni[10] (NS) and the line notation suggested by Kuhn and Scott[11] (KS). Note that all intensities are relative to the strongest line in each group and that the HF ones are valid only for pure LS coupling. They may, therefore, be taken only as a very rough indication for our intermediate coupling case.

The general agreement between the HF and RDF energies is good, particularly for the $2s$-spectator-hole transitions, which agree to 1 eV for all transitions except d^* and e^*. For these, HF and RDF differ by $\sim$7 eV, with the NS value lying half-way between the two. The $2p$-spectator-hole HF transitions are systematically down-

TABLE II. Calculated intermediate-coupling transitions between indicated configurations. Energies, in eV, are adjusted using the measured $K\alpha_1$ energy, as detailed in the text. Intensities are relative to the most intense line of each group. The HF intensities are valid only for *LS* coupling and should be taken as rough indications only.

			Nonrelativistic Hartree-Fock		Relativistic Dirac-Fock		Ref. 10
	Symbol	Transition	Energy	Intensity	Energy	Intensity	Energy
$(1s2s)^{-1}\rightarrow(2s2p)^{-1}$	a^*	$^3S_1\rightarrow{}^3P_2$	8081.5	1.0	8081.1	0.58	8079.6
	b^*	$^3S_1\rightarrow{}^3P_1$	8070.3	0.6	8069.7	0.33	8068.7
	c^*	$^3S_1\rightarrow{}^3P_0$	8061.1	0.2	8060.3	0.12	8059.8
	d^*	$^1S_2\rightarrow{}^3P_1$	8092.9	0	8100.2	0.06	
	e^*	$^1S_0\rightarrow{}^1P_1$	8052.5	0.6	8059.3	1.00	8055.1
	f^*	$^3S_1\rightarrow{}^1P_1$	8029.9	0	8028.8	0.02	
$(1s2p)^{-1}\rightarrow(2p)^{-2}$	a	$^1P_1\rightarrow{}^1D_2$	8084.7	1.0	8080.7	1.00	8082.4
	b	$^3P_2\rightarrow{}^3P_2$	8078.4	0.75	8075.9	0.49	8079.2
	c	$^3P_1\rightarrow{}^3P_2$	8087.6	0.25	8085.6	0.42	8087.2
	d	$^3P_2\rightarrow{}^3P_1$	8060.8	0.25	8058.0	0.19	8062.2
	e	$^1P_1\rightarrow{}^1S_0$	8056.1	0.20	8051.5	0.25	8058.2
	f	$^3P_0\rightarrow{}^3P_1$	8084.2	0.20	8083.0	0.75	8082.1
	g	$^3P_1\rightarrow{}^3P_0$	8074.7	0.20	8072.3	0.25	8076.3
	h	$^3P_1\rightarrow{}^3P_1$	8070.0	0.15	8067.7	0.14	8070.6
	i	$^3P_2\rightarrow{}^1D_2$	8049.9	0	8047.4	0.08	
	j	$^3P_1\rightarrow{}^1D_2$	8059.1	0	8057.1	0.13	
	k	$^1P_1\rightarrow{}^3P_1$	8095.5	0	8091.3	0.05	
	l	$^1P_1\rightarrow{}^3P_2$	8113.1	0	8109.2	0.01	
	m	$^1P_1\rightarrow{}^3P_0$	8100.3	0	8095.9	0.00	

shifted by 2–3 eV relative to the RDF ones. As no such shift is observed in the 2*s*-spectator-hole transitions we suspect that the shift results from the failure of the accepted procedure of scaling the two-electron ζ parameter by the experimental single electron splitting to account completely for the relativistic effects. Intercomparing the three calculated sets of energy levels in Table II, an average scatter of ± 2 eV on the absolute values and ± 1 eV on the splitting between levels is obtained. This supports the claim of KS of 1–2 eV accuracy for their HF-calculated absolute energies, but contradicts their expectation that the calculated splitting between levels is much more accurate.

The RDF-calculated satellite spectrum is compared with the measured one in Fig. 2. The calculated intensities are normalized to the strongest line in each group, which, in the case of the 2*s*-spectator-hole transitions lies outside the energy range of the figure. The calculated positions and intensities follow remarkably well the measured spectrum. Furthermore, the spectrum contains fine structure, some of which was not resolved in earlier studies.[4,7] These features, marked by capitals in Fig. 2 allow more detailed line assignments to be made than the conventional phenomenological four-component resolution presented above. The assignments based on our RDF calculations along with their traditional designations and the earlier assignments of NS, KS, and Demekhin and Sachenko[17] are listed in Table III. The most intriguing conclusion that seems to emerge from Fig. 2 is the assignment of *D*, i.e., α_3, to the $^1P_1\rightarrow{}^1D_2$ 2*p*-spectator-hole transition rather than the $^3P_2\rightarrow{}^3P_2$ one. Note that our assignment is supported not only by the position of the line, the common basis for assignments in all previous studies, but also by the relative intensities of the lines in this region as well as the good alignment of *C* with the $^3P_2\rightarrow{}^3P_2$ line. Furthermore, $E(\alpha_4)$ is now assigned to $^3P_0\rightarrow{}^3P_1$ rather than mainly to $^1P_1\rightarrow{}^1D_2$. Here again the assignment is supported both by position and intensity, *f* being the second strongest line of the 2*p*-spectator-hole group. Such an assignment would be untenable on the basis of HF calculations, because although the energy alignment is good, the *LS* intensity is much too low. Our

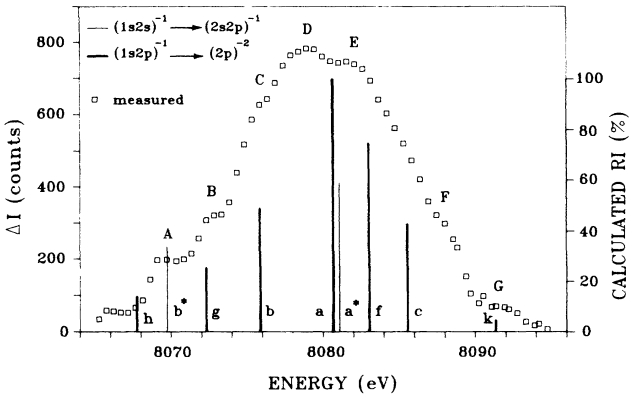

FIG. 2. Comparison of the measured spectrum (□) and calculated relativistic Dirac-Fock transitions $1s^{-1}2s^{-1}\rightarrow 2s^{-1}2p^{-1}$ (thin line) and $1s^{-1}2p^{-1}\rightarrow 2p^{-2}$ (thick line). Note that the lines are separately normalized to the most intense component of each group. The lines are marked by the letter designations of Table II, where the energies and relative intensities (RI) are also listed. The line assignments derived from this figure are listed in Table III.

TABLE III. Transition assignments for the various features detected in the measured spectrum of Fig. 2. Transitions are marked by letter designations from Table II. Note that all calculations except our RDF one are nonrelativistic Hartree-Fock ones. For discussion see text.

Feature	Traditional designation	Present RDF assignment	Ref. 10	Ref. 11	Ref. 17
A	α'	h,b^*	h	h,g	h,d,e^*
B		g			
C		b			
D	α_3	a,a^*	b,a^*	b	c,b^*,g
E	α_4	f	a,f	a,f	a,f
F	α_3'	c	c	c	b,a^*
G		k			

results support the accepted assignment of features A and F to $^3P_1 \rightarrow {}^3P_1$ (in part) and $^3P_1 \rightarrow {}^3P_2$, respectively.

Another important issue is the relative contribution of the $2s$-spectator-hole transitions to the spectrum. The RDF calculations in Fig. 2 show b^* to be in good alignment with $A(\alpha')$, while the nearest $2p$-spectator-hole lines, h and g, are removed by 2 eV to either side of b^*. This would seem to leave b^* as the sole contributor to A. However, the intensity of this feature is such that the three times more intense line e^* should be measurable at $\sim$8059 eV. The second most intense line of this group, a^*, is too close to a to be resolved. Thus the assignment of A to b^* rests solely on the detection or otherwise of e^*. No indication of this line was found in our measurements. Note however, that the increased slope and intensity of the spectrum in this region due to the $K\alpha_1$ line render the detection of satellites extremely difficult as demonstrated by the fact that the medium intensity $2p$ hole lines d and j, expected to lie in this region, were also not detected. We conclude therefore that a small contribution from $2s$-spectator-hole transitions cannot be ruled out. The above discussion is in line with that of KS, who also find no indications for contributions from $2s$-spectator-hole transitions.[18] This is probably a result of the increased Coster-Kronig transition rate for $2s$ holes, which greatly reduces the probability of a radiative $(1s)^{-1} \rightarrow (2p)^{-1}$ transition in the presence of an unfilled $2s$ hole.

Finally, we would like to point out that a phenomenological resolution of the satellite complex, based on features $A-G$, into seven individual lines rather than Parratt's four, is possible in principle. In practice, however, it was found that no convergence of the least-squares routine to reasonable widths, positions, and intensities could be obtained without *a priori* fixing some of the 21 free parameters involved (width, height, and position for each Gaussian). This is hardly surprising in view of the high degree of overlap of the spectrum lines. We feel that such a biased resolution is of no real value. This approach was, therefore, not pursued.

B. Low-energy region

Twenty-eight equidistant points were measured in this region, extending from 8032 to 8043 eV. The measured data are shown in Fig. 3. The contribution from the flanks of the $K\alpha_1$ and $K\alpha_2$ lines was subtracted from the measured values using two Lorentzians to represent each line. The parameters defining the Lorentzians were obtained from the high-resolution measurements of the Cu $K\alpha$ lines reported in Ref. 13. The residuals were then smoothed using a single pass of a five-point parabolic moving window. The results obtained are shown in Fig. 4, along with the statistical mean standard deviations of the original, as-measured data. Clearly no undisputable satellites can be detected in the data above the one standard deviation (σ) limit which corresponds to an intensity of 2×10^{-4} relative to that of the $K\alpha_1$ line. The only possible candidate is the small peak at $\sim$8038 eV. This peak is in good alignment with the photographically recorded line reported by Edamoto[6] at 8038.1 eV, and assigned to a K-$L_3M_{4,5}$ radiative Auger transition by Nigam and Soni.[19] Although having a fairly regular shape incorporating at least five points, the peak intensity of this feature is only 3.2 times σ of the measured data. Thus, the existence of this line in our data is highly tentative. The second low-energy satellite reported by Edamoto at 8044.9 eV was not detected in our experiment.

If, however, the reader is willing to grant the proposed existence and identification of the K-$L_3M_{4,5}$ line in our data, then its width is $\sim$2 eV, which is close to, but

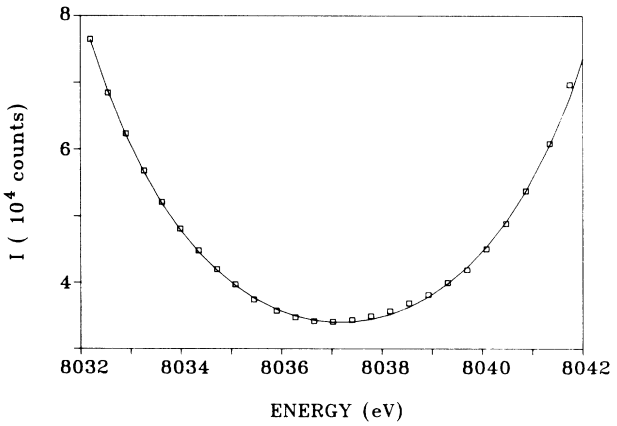

FIG. 3. Measured emission spectrum (□) in the energy region between the $K\alpha_1$ and $K\alpha_2$ lines and the contribution from the flanks of the two diagram lines (——).

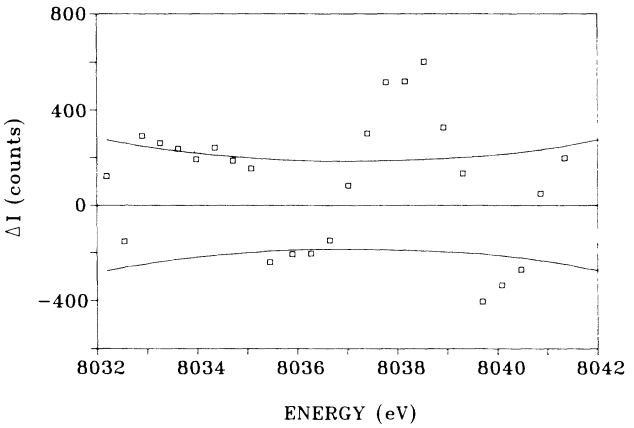

FIG. 4. Measured spectrum of Fig. 3 with the diagram lines' contribution subtracted. The standard deviation in the original data is also shown (——). The only candidate for a satellite line is the small feature at 8038 eV. For a discussion, see text.

somewhat smaller than that of the $K\alpha_1$ line,[12] and its intensity, relative to that of the $K\alpha_1$ line is 5×10^{-4}. This is an order of magnitude smaller than Scofield's[20] theoretical prediction for the *total K-LM* group intensity, but within a factor of 2 of the low-resolution electron capture measurements of Campbell *et al.*[21] Clearly a much more accurate measurement of this line is called for before a meaningful comparison with theory can be attempted.

IV. CONCLUSIONS

We presented here an experimental and theoretical study of the x-ray $K\alpha$ satellite spectrum of copper. While the overall features of this spectrum such as wavelength, total width, and total relative cross section are in good agreement with previous measurements and calculations, a hitherto unresolved fine structure in the spectrum is found. Very good alignment is found between the measured structures and the calculated RDF spectrum of 2*p*-spectator-hole transitions. A possible, though small, contribution of 2*s*-spectator-hole transitions can also not be ruled out. In the region below the $K\alpha_1$ line, radiative Auger lines involving 3*d* electrons are expected. With one possible exception, no such lines were found within our experimental accuracy of 2×10^{-4} of the $K\alpha_1$ line intensity.

Clearly, similar measurements for the neighboring members of the iron-group elements are called for, to support the new line assignments suggested in this study. These measurements should extend to regions closer to the $K\alpha_1$ peak and be preferably of a statistical accuracy an order of magnitude higher than that of the work presented here, a not unreasonable requirement when using high brilliance rotating anode x-ray sources. This will allow the observation of 2*s*-spectator-hole transition lines and the determination of their contribution to the $K\alpha$ satellite spectrum, as well as a measurement of the very weak radiative Auger transition lines expected in the energy region between the $K\alpha_1$ and $K\alpha_2$ lines.

[1]G. Wentzel, Ann. Phys. **66**, 437 (1921).
[2]G. Bradley Armen *et al.*, Phys. Rev. Lett. **54**, 182 (1985).
[3]R. D. Deslattes, R. E. LaVilla, P. L. Cowan, and A. Henins, Phys. Rev. A **27**, 923 (1983); M. Deutsch and M. Hart, Phys. Rev. Lett. **57**, 1566 (1986); K. G. Dyall and R. E. LaVilla, Phys. Rev. A **34**, 5123 (1986).
[4]L. G. Parratt, Phys. Rev. **50**, 1 (1936).
[5]S. I. Salem, A. Kumar, B. L. Scott, and R. D. Ayers, Phys. Rev. Lett. **49**, 1240 (1982); S. I. Salem, A. Kumar, and B. L. Scott, Phys. Rev. A **29**, 2634 (1984); S. I. Salem and A. Kumar, J. Phys. B **19**, 73 (1986).
[6]I. Edamoto, Sci. Rep. Res. Inst. Tohoku Univ. Ser. A **2**, 561 (1950).
[7]H. J. Edwards and J. I. Langford, J. Appl. Cryst. **4**, 43 (1971).
[8]R. D. Richtmyer, Phys. Rev. **49**, 1 (1936).
[9]T. Aberg, in Proceedings of the International Conference on Inner Shell Ionization, Phenomena and Future Applications, USAEC Conference No. 7200404, Atlanta, 1972 (unpublished).
[10]A. N. Nigam and S. N. Soni, Physica **132C**, 407 (1985).
[11]W. J. Kuhn and B. L. Scott, Phys. Rev. A **34**, 1125 (1986).
[12]W. C. Sauder, J. R. Huddle, J. D. Wilson, and R. E. LaVilla, Phys. Lett. **63A**, 313 (1977); J. Hrdy, Czech. J. Phys. B **25**, 597 (1975); **35**, 401 (1985); M. Deutsch and M. Hart, Phys. Rev. B **20**, 5558 (1982).
[13]N. Maskil and M. Deutsch, Phys. Rev. A **37**, 2947 (1988).
[14]Y. Cauchois and C. Senemaud, *Wavelengths of X-Ray Emission Lines and Absorption Edges* (Pergamon, Oxford, 1978).
[15]C. Froese Fischer, Comput. Phys. Commun. **14**, 145 (1978).
[16]I. P. Grant, B. J. McKenzie, P. H. Norrington, D. F. Mayers, and N. C. Pyper, Comput. Phys. Commun. **21**, 207 (1980), B. J. McKenzie, I. P. Grant, and P. H. Norrington, *ibid.* **21**, 233 (1980); I. P. Grant, Int. J. Quant. Chem. **25**, 23 (1984).
[17]V. F. Demekhin and V. P. Sachenko, Bull. Acad. Sci. USSR, Phys. Ser. **31**, 913 (1967).
[18]Note, however, that Kuhn and Scott base their conclusion on the fact that no line is observed experimentally at the position they calculate for the a^* line in Cu and Cr. Both these calculated 2*s* hole spectra seem to be upshifted by about 15 eV relative to the equivalent spectra in the neighboring atoms, and in the case of Cu, also relative to our HF one, which was calculated using the same procedure employed by them. The shift is possibly due to a computational error, which may also be the source of the 4 eV unexplained shift they find in their calculated Ti 2*p*-spectator-hole spectrum.
[19]A. N. Nigam and S. N. Soni, J. Phys. C **13**, 1567 (1980).
[20]H. H. Scofield, Phys. Rev. A **9**, 1041 (1974).
[21]J. L. Campbell, A. Perujo, W. L. Teesdale, and B. M. Millman, Phys. Rev. A **33**, 2410 (1986).